

**$^{24}\text{Mg}(d, \alpha)$  reaction as a test of  $^{22}\text{Na}$  wave functions\***M. J. Schneider<sup>†</sup>*Nuclear Physics Laboratory, Department of Physics and Astrophysics, University of Colorado, Boulder, Colorado 80302  
and Brookhaven National Laboratory, Upton, New York 11973*

J. W. Olness

*Brookhaven National Laboratory, Upton, New York 11973*

(Received 25 August 1975)

The  $^{24}\text{Mg}(d, \alpha)$  reaction has been studied at 26 MeV to test shell model wave functions for the deformed nucleus  $^{22}\text{Na}$ . Excitation functions were first taken to insure that at this energy the  $(d, \alpha)$  reaction on  $^{24}\text{Mg}$  is direct. The distorted-wave Born approximation with optical wells of matched geometry was used. With wave functions based on a Hamiltonian calculated using level energies in a restricted region of the  $s$ - $d$  shell, the data require a roughly constant  $(d, \alpha)$  normalization (within the error of measurement) for 8 of the 10 states studied, indicating the overall correctness of the wave functions. A calculation using a wider range of level energies is less successful. Several new spin suggestions are made and another rotational band in  $^{22}\text{Na}$  is tentatively identified.

[ NUCLEAR REACTIONS  $^{24}\text{Mg}(d, \alpha)$ ,  $E=17$ -26 MeV; measured  $\sigma(E)$ ,  $\sigma(\theta)$ ; compared with shell model predictions; enriched targets, multigap spectrometer. ]

## I. INTRODUCTION

The shell model calculations of Freedom and Wildenthal for  $^{22}\text{Na}$ ,<sup>1</sup> a rotational nucleus with a large deformation, manifest collectivelike properties (e.g., "bands") and have been successful in reproducing various experimental data, such as electromagnetic transition rates, lifetimes, and single-particle spectroscopic factors. Further tests are still useful, though. In particular, the two-particle transfer reaction can be most informative, since coherent interference between nucleon pairs transferred from various configurations provides high sensitivity to the wave functions used in the calculation. With such tests in mind, we have undertaken a study of the  $^{24}\text{Mg}(d, \alpha)$ - $^{22}\text{Na}$  reaction at 26 MeV bombarding energy.

## II. EXPERIMENT

Deuterons were accelerated to 26 MeV by the three-stage double emperor tandem Van de Graaff at Brookhaven National Laboratory. The >99% isotopically enriched  $^{24}\text{Mg}$  target on a carbon backing was 61  $\mu\text{g}/\text{cm}^2$  thick. Outgoing  $\alpha$  particles were analyzed in a multigap spectrograph<sup>2</sup> and detected in aluminum covered Kodak K-1 nuclear emulsions in the spectrograph focal plane. In a preliminary run  $^{24}\text{Mg}(d, \alpha)$  excitation functions were measured from 17 to 26 MeV to determine whether this reaction is truly direct at the higher energy. The excitation functions were taken in a conventional scattering chamber. Representative samples are shown in Fig. 1. The fluctuations in

yield appear to be damped above 20 MeV, so angular distributions were taken at 26 MeV with confidence that the reaction studied is mostly direct for  $d\sigma/d\Omega \geq 10 \mu\text{b}/\text{sr}$ .

Figure 2 shows the  $\alpha$ -particle spectrum observed in the multigap spectrograph at  $\theta_{\text{lab}} = 15^\circ$ . With a resolution of about 33 keV, all states below 4.7 MeV were resolved. Absolute cross sections, believed accurate to  $\pm 20\%$ , were deduced from comparison of the elastic deuteron yield in a monitor detector at  $\theta_{\text{lab}} = 34^\circ$  to the measured elastic cross section.<sup>3</sup> Since the reaction is predominantly direct at this energy, the  $2^+ T=1$  level at 1.952 MeV is forbidden and cannot be populated significantly in this reaction. Therefore the peak at 1.96 MeV was divided between the 1.937 and 1.984 MeV states. All states were identified by their positions on the focal plane. Excitation energies used herein are from Ref. 4.

## III. DISTORTED-WAVE BORN APPROXIMATION CALCULATIONS

Several previous studies have pointed out the importance of matching the geometries of the potential wells for incoming and outgoing particles in order to increase the reliability of distorted-wave Born approximation (DWBA) calculations of reactions with significant momentum mismatch<sup>5</sup> such as the  $(d, \alpha)$  reaction.<sup>6,7</sup> The appropriate Woods-Saxon optical parameters of Perey<sup>8</sup> for 25.9 MeV deuterons on  $^{24}\text{Mg}$  and of Satchler<sup>9</sup> for 28 MeV  $\alpha$  particles on  $^{24}\text{Mg}$  have real "radii" ( $r_0$ ) of 1.15 and 1.7 fm, respectively. Therefore the original data on which both sets are based were refitted

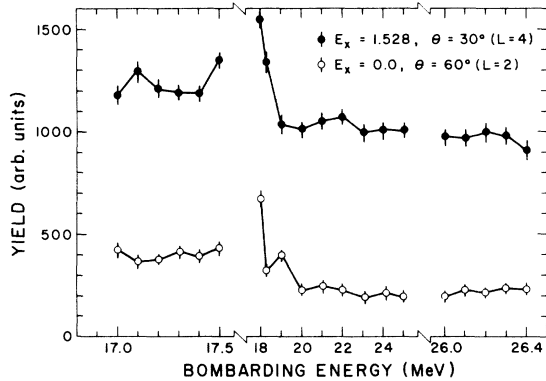


FIG. 1. Excitation functions for  $^{22}\text{Na}$  ground state at  $\theta_{\text{lab}}=60^\circ$  and 1.528 MeV state at  $30^\circ$ . Note variations in bombarding energy scale.

using the code OPTIM.<sup>10</sup> However, the  $\alpha$ -particle well radius could not be reduced below 1.4 fm without the calculated elastic cross section diverging sharply from the experimental result, and similarly the deuteron well radius could not be increased beyond 1.2 fm.

We chose to adopt the suggestion of Stock *et al.*,<sup>5</sup> following the path outlined for several previous  $(d, \alpha)$  investigations,<sup>6,7</sup> by doing the DWBA calculation with matched optical parameters for  $r_0=1.2$ , even though the resulting  $\alpha$  particle elastic scattering<sup>11</sup> is not well reproduced (Fig. 3). The results of this choice are (1) that the finite range correction to the calculated  $(d, \alpha)$  cross sections is reduced from a  $\sim 30\%$  correction to the form

factor for the unmatched set (lines 1 and 2 of Table I) to a  $\sim 5\%$  correction for the  $r_0=1.2$  matched set (lines 3 and 4), and (2) that reproduction of the  $(d, \alpha)$  shapes is improved greatly. This is illustrated in Fig. 4, which shows data for 10 positive parity transitions along with calculations using unmatched and matched optical parameters. The qualitative conclusions of the present study are unchanged whether matched or unmatched optical parameters are used, but the better agreement of the former with data gives confidence that they describe better the physical processes occurring, and hence give more reliable quantitative results.

Microscopic DWBA calculations were done with code DWUCK4<sup>12</sup> for these 10 positive parity states using theoretical transfer amplitudes, and for the 9 other states (Fig. 5) also observed in this experiment. [ $9^\circ(\text{c.m.})$  data have been omitted for some levels because of apparent difficulties due to the large number of inelastic deuteron tracks obscuring the  $\alpha$ -particle tracks on the emulsions.] The cross section calculated by DWUCK4,  $\sigma_{\text{DW}}$ , is given by

$$\sigma_{\text{DW}} = \sum_M |G_{NLSJ} B_{NL}^M|^2, \quad (1)$$

where  $S$ ,  $L$ ,  $J$ , and  $M$  are the transferred spin, orbital, total, and  $z$  component of angular momentum, and  $N$  is the principal quantum number of the transferred pair.  $B$  is the kinematic factor which contains the angular dependence and  $G$  is a struc-

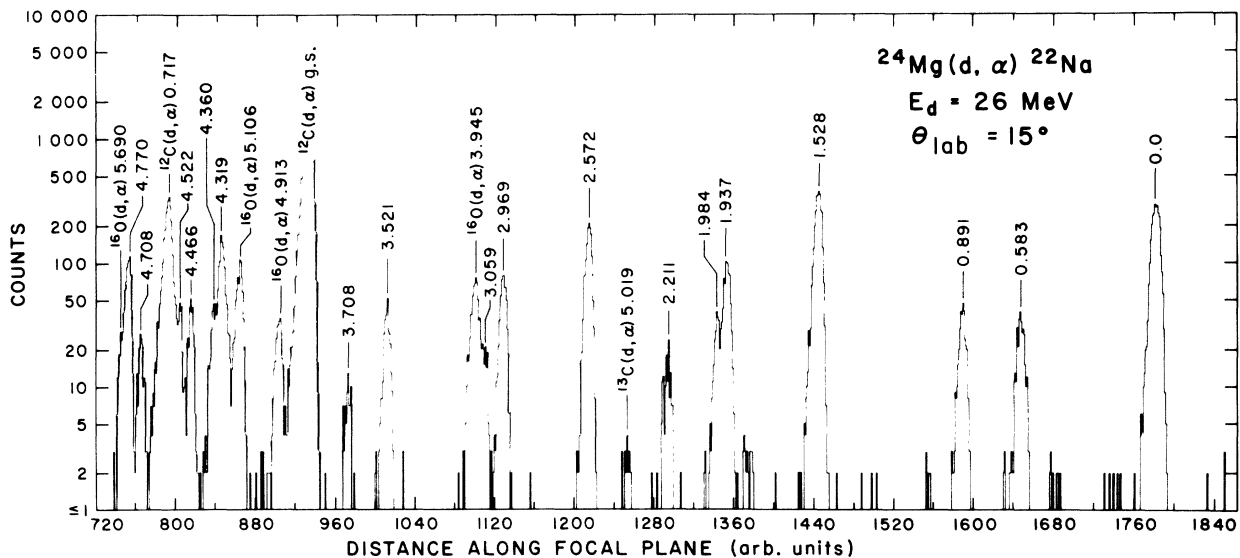


FIG. 2. Spectrum of the  $^{24}\text{Mg}(d, \alpha)^{22}\text{Na}$  reaction at  $\theta_{\text{lab}}=15^\circ$ ,  $E_d=26$  MeV. States of  $^{22}\text{Na}$  are identified by their excitation energies in MeV. Prominent contaminants are also identified. Resolution is about 33 keV.

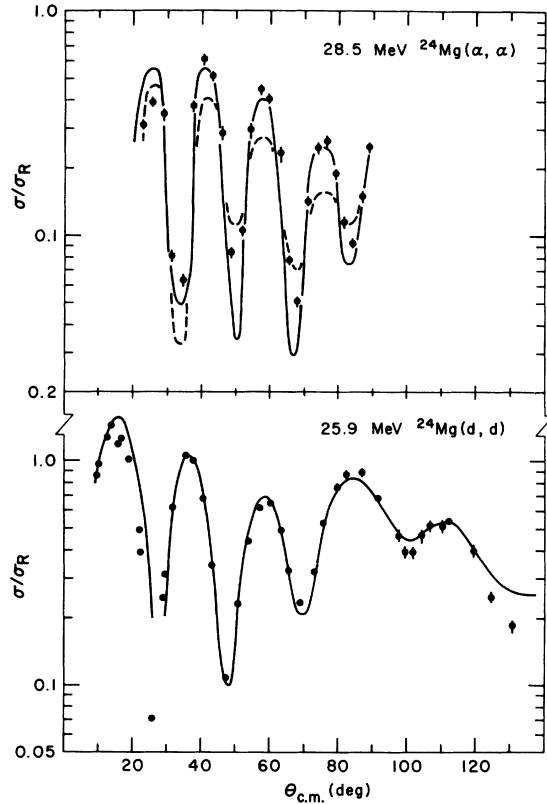


FIG. 3. Elastic scattering of 25.9 MeV deuterons and 28.5 MeV  $\alpha$  particles on  $^{24}\text{Mg}$ . The data are from Refs. 3 and 11, respectively. Where error bars are not shown they are smaller than data points. For deuteron scattering, the accompanying curve is an optical model fit using  $r_0=1.2$  parameters from line 3 of Table I. For  $\alpha$  scattering, the solid curve is a fit using  $r_0=1.4$  parameters (line 2) and the dashed curve uses  $r_0=1.2$  parameters (line 4).

ture factor<sup>13</sup> which can be written

$$G_{NLSJ} = \sum_{\gamma} \beta_{\gamma} G_{\gamma}. \quad (2)$$

TABLE I. Woods-Saxon optical model parameters used in DWBA calculations. All well depths are in MeV and radii and diffusivities in fm.  $W_s$  is the surface imaginary well depth and  $W_v$  is the volume imaginary well depth.

Channel	Source	$V_0$	$r_0$	$a$	$4W_s$	$W_v$	$r_i$	$a_i$	$V_{so}$	$r_{so}$	$r_c$
$d-^{24}\text{Mg}$	Ref. 8	76.63	1.151	0.746	47.76	...	1.156	0.93	...	...	1.2
$\alpha-^{22}\text{Na}$	Present work	198.09	1.4	0.592	...	22.52	1.574	0.126	...	...	1.3
$d-^{24}\text{Mg}$	Present work	72.5	1.2	0.746	48.08	...	1.223	0.861	...	...	1.2
$\alpha-^{22}\text{Na}$	Present work	182.3	1.2	0.737	...	34.24	0.991	0.797	...	...	1.3
Bound nucleons		a	1.25	0.65	...	...	...	...	25	1.25	1.3

<sup>a</sup> Dependent upon separation energy of bound state.

The  $\beta_{\gamma}$  are the spectroscopic amplitudes for proton-neutron configuration  $\gamma$  (these were supplied by Wildenthal<sup>1</sup> for this study) and  $G_{\gamma}$  are other configuration-dependent quantities.

$\sigma_{\text{DW}}$  is related to experimental cross section,  $\sigma_{\text{exp}}$ , by the equation

$$\sigma_{\text{exp}} = \frac{N(d, \alpha) \sigma_{\text{DW}}}{2J+1}, \quad (3)$$

where  $N(d, \alpha)$  is the  $(d, \alpha)$  reaction normalization. This number is strongly dependent on how the form factor is calculated and other parameters of the DWBA calculation. The geometry of the form-factor potential well is given in Table I. Its depth was calculated to bind the proton and neutron at the proper separation energy for each  $^{22}\text{Na}$  state, assuming the excitation energy to be shared equally between proton and neutron. The rms radius of the  $\alpha$  particle was taken as 1.7 fm. The distorted waves for the deuteron and  $\alpha$  particle were calculated with the standard nonlocality correction,<sup>12</sup> and the finite range correction was taken to be of the Hulthén form with parameter  $R=0.4$  fm.

#### IV. SHELL MODEL CALCULATIONS

Two shell model calculations were tested: those of Priedom and Wildenthal,<sup>1</sup> and those of Wildenthal and Chung.<sup>14</sup> In brief, both use an  $^{16}\text{O}$  core, the entire  $1s-2d$  shell model space, and an empirical interaction based on Kuo's matrix elements as a starting point. In the former calculation, the two-body matrix elements were adjusted to reproduce as well as possible 72 level energies in the  $A=18-22$  region. In the latter calculation a more global point of view was taken and the Hamiltonian was adjusted to best reproduce level energies from  $A=17$  to 26. As will be seen below the global point of view did not benefit the  $^{22}\text{Na}$  calculation.

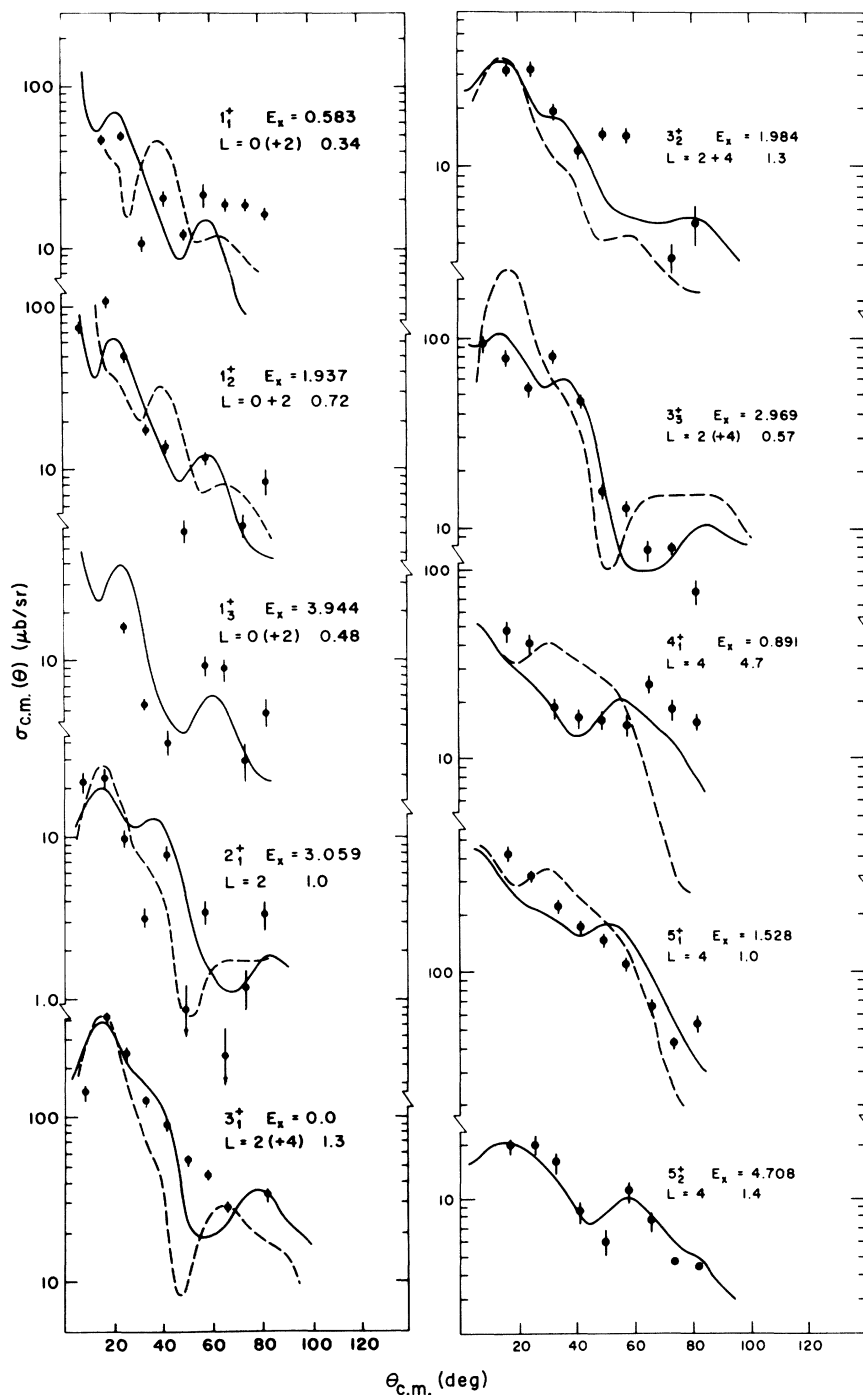


FIG. 4.  $^{24}\text{Mg}(d, \alpha)$  angular distributions leading to 10 of the positive parity  $^{22}\text{Na}$  states whose shell model wave functions have been calculated. Curves are cross sections predicted by DWBA using transfer amplitudes based on these wave functions. Dashed curves use unmatched optical parameters (lines 1 and 2 of Table I) and solid curves use matched parameters (lines 3 and 4). Excitation energies are given in MeV and allowed  $L$  values are shown. Parentheses designate  $L$  values whose contributions are negligible. Numbers following  $L$  values are  $(d, \alpha)$  normalizations divided by the average  $(d, \alpha)$  normalization for eight states,  $N = 580$  (see text and Table II). Possible  $4_2^+$  state is shown in Fig. 5.

## V. COMPARISON OF CALCULATIONS AND EXPERIMENT

The shapes of the  $(d, \alpha)$  angular distributions (Figs. 4 and 5) are generally well reproduced by

DWBA with matched optical parameters. Some of the disagreements appear to be manifestations of a frequently seen shortcoming of the DWBA description, in that the angular distributions resem-

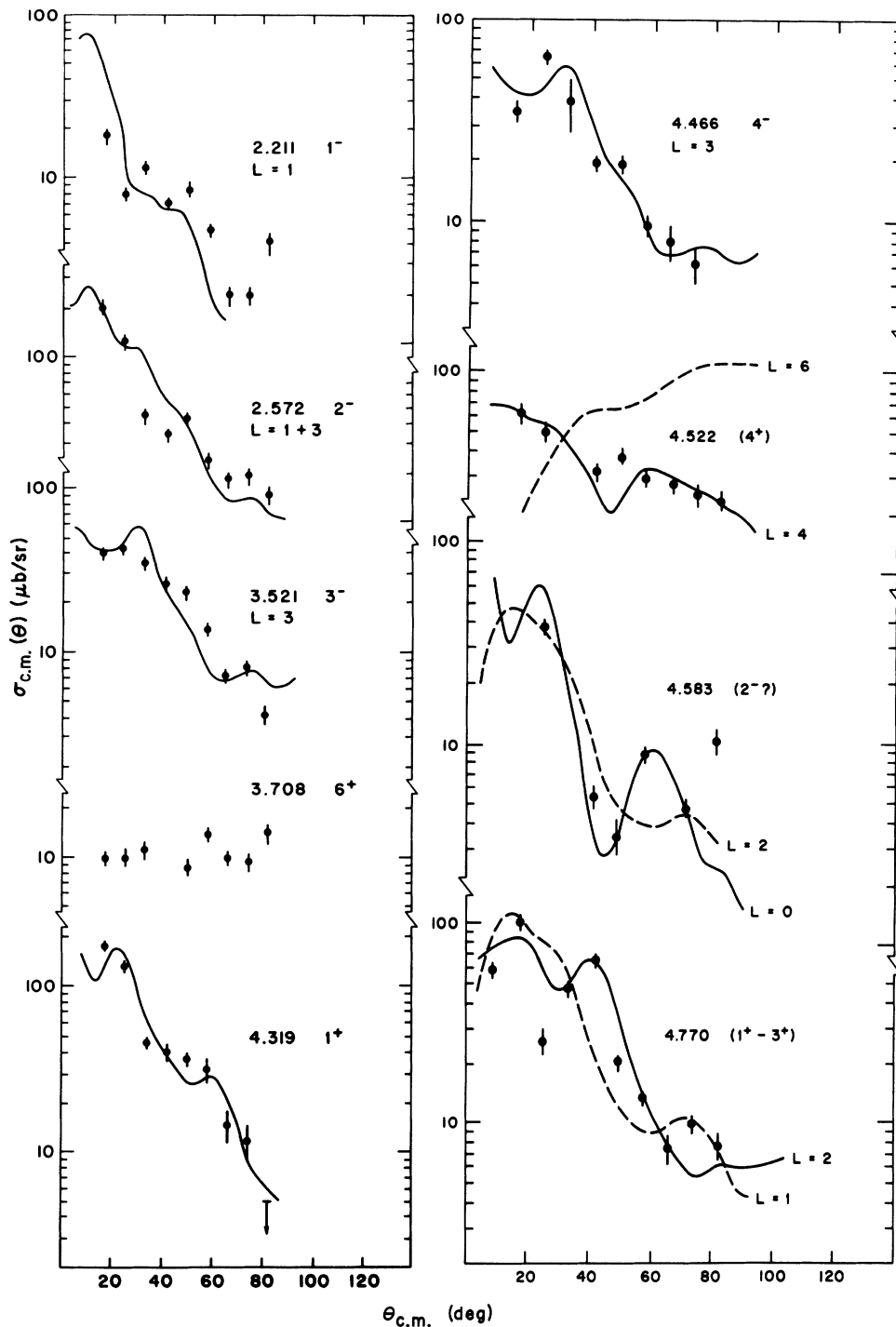


FIG. 5.  $^{24}\text{Mg}(d, \alpha)$  angular distributions for nine other states of  $^{22}\text{Na}$  populated in this experiment. Curves are DWBA calculations normalized to the data for best fit. For negative parity states, calculations use  $(d_{5/2}, p_{3/2})$  pickup coupled to the  $L$  value(s) shown.

ble those seen in other regions of the Periodic Table, sometimes with multiple shapes for a given  $L$  value, and hence not always in agreement with calculations. (These similarities across many shells and variations for the same  $L$  value in two-particle transfers will be the subject of a future paper.<sup>15</sup>)

Since in the direct  $(d, \alpha)$  reaction  $S=1$  and (in the zero-range approximation) the parity change is  $(-1)^L$ , positive (negative) parity states will be populated by even (odd)  $L$  transfers satisfying  $J+1 \geq L \geq J-1$ . This explains all  $L$  values given in Figs. 4 and 5.  $L$  values in parentheses contribute little or nothing to the shapes shown.

The calculated cross sections shown in Fig. 4 are based on the Preedom-Wildenthal<sup>1</sup>  $(d, \alpha)$  transition amplitudes. With the calculational mode described above, a  $(d, \alpha)$  reaction normalization  $N(d, \alpha) = 580$  was found by comparison of predicted and experimental cross sections for 8 of the 10 positive parity states in Fig. 4. The other two states demonstrated poor agreement of prediction and experiment, as is discussed below, and were not included in calculating  $N$ . The numbers accompanying the 10 curves in Fig. 4 are the factors by which  $N = 580$  had to be multiplied to give curves of the magnitudes shown. Six of these numbers lie between 0.57 and 1.33, i.e., within  $\pm 43\%$  of 1.0. The uncertainty in determining  $N$  from any one angular distribution is of the order of 33%, and hence for these six states any errors in the shell model calculation are almost obscured by the

“noise” in our measurement process. We consider this to indicate a successful calculation. If several  $\pi$ - $\nu$  configurations contribute to a transition, the total  $(d, \alpha)$  cross section varies linearly with the magnitude of any single contribution (for small variations). Hence one can say qualitatively that all components of these six wave functions appear to be accurate to better than 43%.

A possible exception, however, is the  $3_3^+$  state, with which the shell model calculation has had some difficulty. It is at least six times weaker in  $d$ -wave single-particle pickup than predicted, and its lifetime is  $\frac{1}{30}$  of the calculated value. Also, it has roughly half the predicted  $(d, \alpha)$  strength (using  $N = 580$ ) but about 2.5 times the predicted  $l=2$  ( $^3\text{He}, d$ ) strength. Apparently the shell model calculation overestimates the  $d$ -shell population of this level.

The first  $1^+$  state, at 0.583 MeV, requires our empirical  $(d, \alpha)$  normalization,  $N = 580$ , to be multiplied by 0.34 for agreement between calculation and experiment. We have no ready explanation of why the predicted magnitude of this primarily  $(d_{5/2})^2$  transition should be so much larger than the experimental value, although the present result combined with the overestimation (by a factor of 3) of the strength of the electromagnetic transition from this level to the ground state casts doubt on the shell model description of this state. We note that the magnitudes of the  $(d, \alpha)$  transitions to the second and third  $1^+$  states are well predicted, making it unlikely that some configurations

TABLE II.  $N(d, \alpha)$  [ $(d, \alpha)$  reaction normalization] required for best agreement of DWBA (using calculated transfer amplitudes based on shell model) and experiment.

State	$E_x$ (MeV)	Calculation of Ref. 1 <sup>a</sup>		Calculation of Ref. 14 <sup>a</sup>	
		$N$	$N/580$	$N$	$N/750$
$1_1^+$	0.583	(200)	0.34	(125)	0.17
$1_2^+$	1.937	420	0.72	(110)	0.15
$1_3^+$	3.944	280	0.48	250	0.33
$2_1^+$	3.059	620	1.1	680	0.91
$3_1^+$	0.0	730	1.25	770	1.0
$3_2^+$	1.984	780	1.3	1090	1.5
$3_3^+$	2.969	330	0.57	320	0.43
$4_1^+$	0.891	(2740)	4.7	1290	1.7
$4_2^+$	(4.522)	(5700)	9.8		
$5_1^+$	1.528	600	1.0	820	1.1
$5_2^+$	4.711	840	1.4	(2300)	3.1
Average $N$		580		750	

<sup>a</sup> Parentheses indicate that  $N$  was excluded from calculation of average  $N$ .

have been neglected. The other pathological cases in this experiment are the  $4^+$  states, predicted (using  $N=580$ ) to have  $\frac{1}{10}-\frac{1}{5}$  of their actual strengths. No configurations other than the predicted ( $d_{3/2}-d_{5/2}$ ) configuration are likely to contribute to these transitions, since  $(l_j)^2$  transfer is forbidden for even spin final states. Available experimental data on the  $4^+$  states agree with shell model calculations, raising the possibility that some perversity of the  $(d, \alpha)$  reaction might be responsible for the disagreement observed herein.

The angular distributions calculated using the latter<sup>14</sup> (Wildenthal-Chung) shell model calculations are largely unchanged in shape from those shown in Fig. 4. The single exception is for the  $3^+$  state at 1.984 MeV, for which the latter calculations predict relatively more  $L=4$  and hence yield better reproduction of the data. The shortcomings of this calculation are manifested in the greater spread of  $N(d, \alpha)$  required to fit nine states, as indicated in Table II. Although the normalization for the  $4_1^+$  state becomes comparable with that for other states, two  $1^+$  states are strongly overpredicted and the  $5_2^+$  state is underpredicted. For seven states the average value of  $N$  using the latter shell model calculation is 750, with the extremes within  $\pm 72\%$  of this value.

#### VI. OTHER STATES OF $^{22}\text{Na}$

Figure 5 shows angular distributions for four known negative parity states and the five remaining states populated in this experiment. DWBA calculations for the former for likely configurations give reasonable agreement with experimental angular distributions.

The weakness and apparently nondirect nature of the transition to the  $6^+$  state at 3.708 MeV may be due to its predicted<sup>1</sup> multiparticle multihole nature. This structure is likely to be the reason for its nondirect angular distribution in all reactions in which it appears.<sup>16-18</sup> The state at 4.319 MeV is better reproduced by  $L=0+2$  than by any other single  $L$  or combination of  $L$  values, reinforcing its  $1^+$  assignment.<sup>4,16</sup> The 4.770 MeV state, previously assigned  $0^+-4^+$ ,<sup>17</sup> is substantially better fit by  $L=2$  than any other  $L$  and so we narrow its assignment to  $(1-3)^+$ .

A state near 4.522 MeV is populated in the  $(d, \alpha)$  reaction with a maximum cross section of 60  $\mu\text{b}/\text{sr}$ , suggesting that it is not the  $7^+$  state previously seen<sup>19-21</sup> at this excitation, since a  $7^+$  state would be weakly populated in a pickup reaction on an  $s-d$  shell nucleus. Furthermore, its angular distribution appears to be  $L=4$ . We therefore suggest it as a candidate for the  $4_2^+$ ,  $T=0$

state, predicted<sup>1</sup> to lie at 4.34 MeV, but not previously identified. This state is also predicted<sup>1</sup> to be a member of the  $K=1$  band based on the  $\frac{3}{2}^+[211], \frac{1}{2}^+[211]$  configuration whose bandhead is the  $1^+$  state at 1.939 MeV.<sup>18</sup> The  $2^+$  member of this band appears to lie at 3.059 MeV,<sup>18</sup> and our tentative identification of the  $4^+$  member eliminates the uncertainty<sup>17,18</sup> in location of the  $3^+$  member by identifying it with the 2.969 MeV rather than 4.770 MeV level, in agreement with shell model<sup>1</sup> and rotational<sup>18</sup> calculations. The former predict that the  $4_2^+$  state will decay most strongly to the  $2^+$  state at 3.059 MeV. However, no  $\gamma$  ray of energy near 1463 keV is seen in the  $^{10}\text{B}(^{14}\text{N}, d\gamma)$  reaction.<sup>19</sup> This may merely mean that the  $4_2^+$  state is not populated very strongly in  $^{10}\text{B}(^{14}\text{N}, d)$  while it is in  $^{24}\text{Mg}(d, \alpha)$ . We note further that in previous  $^{19}\text{F}(^3\text{He}, p\gamma)$  investigations<sup>4,21,22</sup> this  $\gamma$  ray could have been obscured by a  $^{19}\text{F}$  transition of 1.458 MeV.

The Penn group has seen both positive<sup>18</sup> and negative<sup>16</sup> parity states near 4.583 MeV excitation. The angular distribution of the state at this excitation populated in  $(d, \alpha)$  is slightly better reproduced by  $L=0$  than  $L=1$ , suggesting positive parity, but the apparent presence of a close doublet here deserves further attention.

#### VII. SUMMARY AND CONCLUSIONS

We have tested two shell model calculations for wave functions of 10 positive parity states in  $^{22}\text{Na}$  by studying the  $^{24}\text{Mg}(d, \alpha)$  reaction at 26 MeV. The first calculation used level energies in the  $A=18-22$  region to derive its Hamiltonian, while the second calculation used energies of  $A=17-26$  nuclei. Both calculations reproduced angular distribution shapes well, but the first calculation, which considered level energies over a smaller mass region, gave a more consistent normalization (usually within the error of measurement) for the states studied. (The dependence of this normalization on several weak states and on one state where the shell model calculation has an apparent fault diminishes the significance of its exact value.) The range of normalizations required for seven states with the second calculation was about twice as large. The first calculation required large extremes in normalization for the first  $1^+$  state and the  $4^+$  states. These difficulties have not been foreshadowed by other disagreements between theory and experiment, and we have no ready explanation of their origin. It should be mentioned, however, that there are several reservations concerning the DWBA applied to the  $(d, \alpha)$  reaction as a test of  $^{22}\text{Na}$  wave functions. Firstly, form factors were calculated in spheri-

cal, rather than deformed, wells. Secondly, the adequacy of the optical model itself for light deformed nuclei is questionable (although the well-matching procedure, not previously applied below mass 48, may have strengthened the optical model here). Finally, the possibility of two-step processes in this collective nucleus has not been considered. Although apparently important in the  $^{98}\text{Mo}(d, \alpha)$  reaction at 17 MeV bombarding energy,<sup>23</sup> two-step processes have not generally been found necessary in  $(d, \alpha)$ . Single-step DWBA can be applied to  $(d, \alpha)$  successfully in a consistent fashion over a wide range of masses.<sup>7</sup> Multistep analysis of present data would be interesting, but is outside the scope of the present paper, which, we note, does not contain a large number of severe anomalies that would cast doubt on its conclusions.

The above reservations could conceivably be

responsible for some of the disagreements between theory and experiment observed herein. In spite of them, the over-all agreement in this first-order comparison is quite pleasing. The present  $(d, \alpha)$  experiment has succeeded in narrowing the choice of spins for the 4.770 MeV level and has identified an apparent  $4^+$  state near 4.522 MeV. It seems likely that this state is a member of a third positive parity rotational band, but further  $\gamma$  spectroscopy is needed to confirm this assignment.

We are grateful to B. H. Wildenthal for providing us with deuteron pickup amplitudes and information on their use. P. D. Kunz is also to be thanked for discussions concerning code DWUCK4. The photographic emulsions were expertly scanned by A. R. Trent and M. E. Gonzales of the University of Pittsburgh Nuclear Physics Laboratory.

\*Work supported in part by the U.S. Energy Research and Development Administration.

†Present address: Krasdale Foods Corporation, Bronx, New York 10474.

<sup>1</sup>B. M. Freedom and B. H. Wildenthal, Phys. Rev. C 6, 1633 (1972); B. H. Wildenthal (private communication).

<sup>2</sup>H. A. Enge and W. W. Buechner, Rev. Sci. Instrum. 34, 155 (1963).

<sup>3</sup>H. R. E. Tjin a Djie, F. Udo, and L. A. Ch. Koerts, Nucl. Phys. 53, 625 (1964).

<sup>4</sup>J. W. Olness, W. R. Harris, P. Paul, and E. K. Warburton, Phys. Rev. C 1, 958 (1970).

<sup>5</sup>R. Stock, R. Bock, P. David, H. Duhm, and T. Tamura, Nucl. Phys. A104, 136 (1967).

<sup>6</sup>M. J. Schneider and W. W. Daehnick, Phys. Rev. C 4, 1649 (1971).

<sup>7</sup>R. M. Del Vecchio and W. W. Daehnick, Phys. Rev. C 6, 2095 (1972).

<sup>8</sup>C. M. Perey and F. G. Perey, Phys. Rev. 152, 923 (1966).

<sup>9</sup>G. R. Satchler, Nucl. Phys. 70, 177 (1965).

<sup>10</sup>D. H. Zurstadt, University of Colorado (unpublished).

<sup>11</sup>J. Kokame, K. Fukunaga, N. Inoue, and H. Nakamura, J. Phys. Soc. Jpn. 20, 475 (1965).

<sup>12</sup>P. D. Kunz, Univ. of Colorado (unpublished).

<sup>13</sup>N. K. Glendenning, Phys. Rev. 137, B102 (1965).

<sup>14</sup>W. Chung and B. H. Wildenthal, Bull. Am. Phys. Soc. 20, 600 (1975); B. H. Wildenthal and W. Chung, *ibid.* 20, 600 (1975); B. H. Wildenthal (private communication).

<sup>15</sup>M. J. Schneider (unpublished).

<sup>16</sup>J. D. Garrett, R. Middleton, D. J. Pullen, S. A. Andersen, O. Nathan, and O. Hansen, Nucl. Phys. A164, 449 (1971).

<sup>17</sup>J. D. Garrett, H. T. Fortune, and R. Middleton, Phys. Rev. C 4, 1138 (1971); J. D. Garrett, Ph.D. thesis, University of Pennsylvania, 1970 (unpublished).

<sup>18</sup>J. D. Garrett, R. Middleton, and H. T. Fortune, Phys. Rev. C 4, 165 (1971).

<sup>19</sup>M. J. Schneider and J. W. Olness, Bull. Am. Phys. Soc. 17, 529 (1972); (unpublished).

<sup>20</sup>J. N. Hallock, H. A. Enge, A. Sperduto, R. Middleton, J. D. Garrett, and H. T. Fortune, Phys. Rev. C 6, 2148 (1972).

<sup>21</sup>R. M. Freeman, F. Haas, B. Heusch, J. Fernandez Castillo, J. W. Olness, and A. Gallman, Phys. Rev. C 8, 2182 (1973).

<sup>22</sup>F. Haas, R. M. Freeman, J. Fernandez Castillo, and A. Gallman, Phys. Rev. C 8, 2169 (1973).

<sup>23</sup>W. R. Coker, T. Udagawa, and J. R. Comfort, Phys. Rev. C 10, 1130 (1974).